International Journal in Physical and Applied Sciences
Volume 07 Issue 1, January 2020 ISSN: 2394-5710 Impact Factor: 4.657
Journal Homepage: http://ijmr.net.in, Email: irjmss@gmail.com
Double-Blind Peer Reviewed Refereed Open Access International Journal

EFFECT OF DOPANT CONCENTRATION IN SOL–GEL DERIVED AZO LAYER ON THE EFFICIENCY OF SOLAR CELL WITH ACTIVE LAYER POT: $PC_{71}BM$.

Hayder A. Hasan*, Khalid I. Ajeel*

Department of physics, college of education, Basrah University

Abstract

Organic solar cells based on Poly O-Toluidine (POT):$PC_{71}BM$ with an inverted structure have been fabricated using aluminum doped ZnO (AZO) as their electron transport layer, which was prepared by sol-gel method with Isopropyl alcohol as the solvent. The effect of Al concentration on the surface morphology and optical properties of AZO layer were investigated by atomic force microscopy, scanning electron microscopy, X-ray diffraction and UV–visible. The experimental results indicate that Al concentration has major influence on the grain size and only minor influence on crystallite size, leading to different surface morphology for different doping concentrations. Doping at high concentration produces higher charge carrier density, which may be also influenced by the surface morphology. The effects of Al concentration in AZO layer were also observed in the J-V (current density-voltage) of the fabricated solar cells. The solar cell using AZO layer with doping concentration of 0.7 wt% shows the best J-V characteristics with the highest conversion efficiency (1.14%). These characteristics seem to be correlated with the properties of AZO layer and its interface with the active layer.

1. Introduction

In recent years, the inverted device geometry is an attractive concept to improve the longevity, because it only uses electrode and interface materials with a higher work function and significantly improved air stability. For efficient inverted bulk heterojunction (BHJ) solar cells, transparent and conductive interfacial materials, which are inserted between transparent conductive electrode and photoactive layer, are required. The role of this electron extraction layers is not only to form an electron selective layer but also to form an electrical contact to a less air sensitive high work function metal, e.g. Ag or Au. Recently a thin layer (10–40 nm) of solution-processed sol–gel titanium oxide [1] or zinc oxide [2,3] has been successfully applied as an interfacial layer in the normal and inverted geometry. These materials are transparent in the visible light spectrum but absorb ultraviolet (UV) light. The use of metal oxide layer may give an advantage in preventing the active layer from the unwanted oxidation due to UV light radiations of the sunlight and humidity exposure [4]. The use of ZnO layer in solar cell with inverted structure, such as in FTO/ZnO/P3HT:PCBM/MoO_3/Ag structure configuration, improves charge carrier extraction as a result of the lowering of Fermi energy level at the cathode [5]. Moreover, Manoharan et al. have also reported the observation of charge transfer between Poly(aniline-co-o-toluidine) and ZnO, indicating the role of ZnO as an electron acceptor layer [6]. After this report, many studies concern the role of ZnO and its nano-structured layer on exciton dissociation and charge carrier extraction

[7]. ZnO is one type of non-stoichiometric metal oxides with native defect such as zinc interstitial and oxygen vacancies, which intrinsically forms the n-type semiconductor [8]. The conductivity of ZnO thin film can be improved by additing of a small amount of metal ions, such as Al, Ge, etc. [9]. Aluminum doped ZnO (AZO) is one of the most studied ZnO film for TCO applications, which is consider able prospective material as a substitute of Sn-doped In_2O_3 (ITO).Similar to the undoped ZnO, AZO can be prepared by various methods such as direct current (DC) magnetron sputtering, solvothermal, self-assembly monolayer and sol–gel process [10]. The preparation method by sol–gel process is attractive because it is possible for fabrication of large area TCO with more simple and inexpensive equipments in comparison to other methods [11]. For the preparation of AZO by sol–gel process, aluminum chloride ($AlCl_3$) and aluminum nitrate $Al(NO_3)_3$ are commonly used as the precursor of Al dopant ion[12]. The presence of Al dopant may increase the density of states(DOS) near Fermi energy level and thus increases charge carrier density, leading to the increase in electrical conductivity [12,13].By using AZO thin film instead of the undoped ZnO layer, one may thus expect the reduction of the solar cell impedance and thus the improvement in solar cell performance. Moreover, because AZO has relatively larger charger carrier concentration and charger carrier mobility in comparison to the organic transport layer, the solar cell performance is also almost unaffected by the layer thickness variation [14]. However, the effect of using doped ZnO layer on the performance of organic solar cell has not been investigated in detail. Therefore, in this paper, we present the effect of doping concentration of AZO layer on the characteristics of organic solar cells with bulk heterojunction of Poly O-Toluidine:$PC_{71}BM$ as their active layer. The characteristics of those solar cells were investigated by the current density–voltage (J–V).The present experimental result shows the relationship between the Al dopant concentration on the J–V characteristics, which will be discussed in the following sections.

2. Experimental methods

Al doped ZnO synthesis: Zinc oxide (ZnO) is prepared by Sol-Gel technology by dissolving 0.5 M zinc acetate di-hydrate (from Aldrich) in isopropyl alcohol and then diethanol amine was added as the stabilising agent. The molar ratio of zinc acetate di-hydrate to diethanol amine is at 1:1. $AlCl_3$ was added (in the form of $AlCl_3$ with four different ratios, i.e., 0, 0.3, 0.7 and 1.2wt%) into the solution and the mixture solution was then stirred on a magnetic stirrer for about 1h until the solution changed to a clear transparent solution. The prepared AZO sol was used to produce AZO layer which used as receiver for fabrication of the electron transport layer.

Active layer synthesis: To prepare poly O-Toluidine, add 0.05 mol of O-Toluidine (OT) to 200 ml of hydrolyric acid (1.0M HCl). It leaves it for (24hr) on the mechanical mixer and then cools to (0-5°C) in an ice bath. Add (0.025 mol), ammonium persulfate ($(NH_4)_2S_2O_8$) to (40ml) of 1.0 M hydrochloric acid. It is placed on the magnetic stirrers for (3hr) and cooled to (0-5°C). Then put in a separating funnel. The oxidizing agent drops are allowed to slowly descend on the monomer solution (since the reaction is exothermic). After the reaction is completed, the solution is left on the mechanical mixer for three hours at a temperature (0-5 °C). After the polymerization process is completed, the product is filtered by Bochner funnel connected to a vacuum pump. Then

wash with 1M HCl acid until the streaming becomes colorless. Then wash with methanol, acetone, and distilled water several times until the filtrate becomes colorless each time. Then the precipitate was placed inside a thermal oven at (50^{o}C) for a period of (24hr), thus obtaining the poly O-Toluidine polymer doped with HCl acid. The final product was washed with 400ml of NH_4OH 10.0M at room temperature and stirred for 24hr. Then wash it with distilled water for a period of (24hr) and continue with the process of magnetic mixing followed by filtration and drying, then place the precipitate inside a thermal oven (50ºC) for a period (24hr).

After the synthesized poly O-Toluidine by chemical polymerization method, the poly O-Toluidine powder was added to N-Methyl-2-pyrrolidone (NMP) solvent and mixed under constant stirring at room temperature. The $PC_{71}BM$ polymer was dissolved with 1,2-dichlorobenezene (o-DCB) at a concentration (20mg / ml). The O-Toluidine was mixed with the $PC_{71}BM$ polymer in volumes (1:1). After completing the mixing process, the polymer was filtered, then the mixture was deposited on either silicon, interdigitated finger, or glass substrates as a thin films using spin coating.

2.2. Characterization of materials and device fabrication

Device Fabrication: Fig. (1) schematic shows inverted geometry organic solar cells. The inverted organic solar cell comprises of an active layer of POT: $PC_{71}BM$ sandwiched between a transparent conductive oxide (TCO) coated glass as a cathode (ITO) and a top metal layer as an anode. ITO on glasses substrate with ZnO and Al doped ZnO electron extraction layers were used for the fabrication of the inverted organic solar cells under identical processing conditions. Using this solution with 0.5M zinc acetate di-hydrate and the spin coating rotation speed of 1000 rpm for 30s, the thickness of Al-ZnO layers were (41.6, 42.8, 39.8, 40.2nm) for thin film (0.0,0.3, 0.7, 1.2 wt.% Al) respectively. The thin films of this solution were then subjected to annealing to 500^{o}C using a thermal oven in order to convert the solution into Al-ZnO. POT: $PC_{71}BM$ was then spin coated on the top of Al-ZnO layer on ITO substrate glass, the thickness of layer was 136.3 nm. The films were then annealed to 100^{o}C in order to improve the contact between the polymer and Al-ZnO layer. The PEDOT: PSS is deposited on a POT: $PC_{71}BM$ layer with spin coating technology and annealing up to 100 ℃ as a hole transport layer. The thickness of layer was 104.7nm. Finally, an electrode consisting Au was thermally evaporated under vacuum of ~ 1×10^{-5}torr.

Characterization: Current–voltage characteristics of OPV devices were conducted on the computer controlled Keithley model 2400 digital source meter. Illumination was provided by a solar simulator with AM1.5G spectra at100 mW/cm^2. The UV- vis absorption spectra of the polymer films were recorded on Varian 50 scan UV-visible spectrophotometer. The blend structures were investigated by multipurpose X'Pert PHLIPS X-Ray defractometer (MPD), and the film thickness was determined using M2000V (J.A. Woollam Co., Inc.) spectroscopic ellipsometer, operating in the wavelength range 370-1000 nm. The scanning electron microscope (SEM) and the tapping mode atomic force microscope (AFM) images were recorded using FEI™ Nova Nano SEM and Vecco Nanoscope III AFM, respectively.

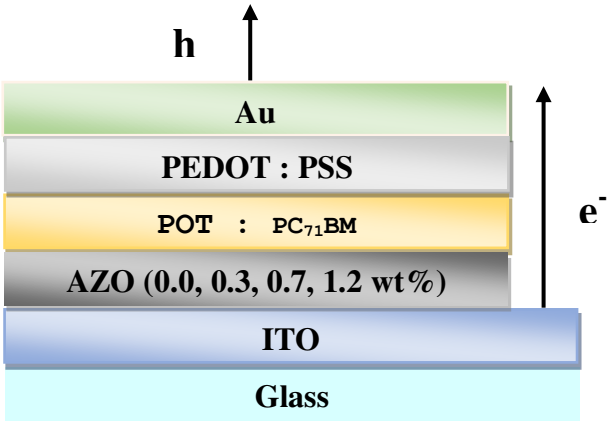

Fig.1: Schematic structure of inverted type of organic solar cells based on POT: $PC_{71}BM$ with AZO a sit selectron transport layer.

3. Results and discussions

Figs. 2 shows the AFM images of the ZnO and AZO layers with various concentrations of Al doping, namely 0.3, 0.7 and 1.2 wt%. It seems that the surface morphology is affected by the Al concentration. Increasing the doping concentration seems to reduce the grain size but increase the appearance number of bulges on the surface. This characteristic may be related with the increase in ZnO grain packing density with increasing dopant concentration, resulting in the reduction of ZnO grain size, as also already reported [15,16]. The surface morphology of the 0.7 wt% seems to have more flat surface with less bulge structures.

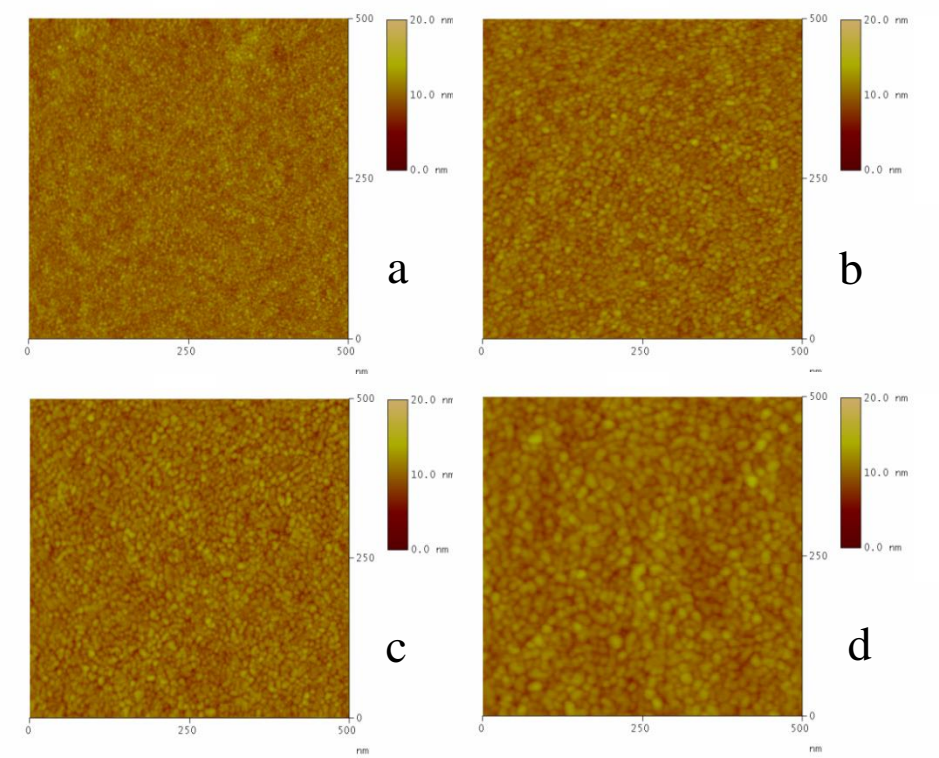

Fig. 2: Atomic force microscopy (AFM) images of (a) Undoped, (b) Al-ZnO -0.3wt%, (c) 0.7wt%, and (d)1.2wt%.

Figure 3(a), (b), (c) and (d) shows the SEM of the surface of Al doped ZnO thin films with different Al concentration (0, 0.3, 0.7 and 1.2 at wt.%) for constant substrate temperature. SEM image at normal incidence shows the microstructure of Al-ZnO consisting of many spherical shaped crystalline particles. The grains more or less cover the substrate surface uniformly. However, Al-ZnO film shows particles with off-spherical shape. Thus, Al doping seems to have modified the shape of the grains. The microstructure is found to be uniform with compact interconnected grains. Also the film appears to have less porosity than pure ZnO film indicating that the film became denser with Al incorporation [17].The SEM image shows that the average grain size is decreased with increasing of Al-doping[18].

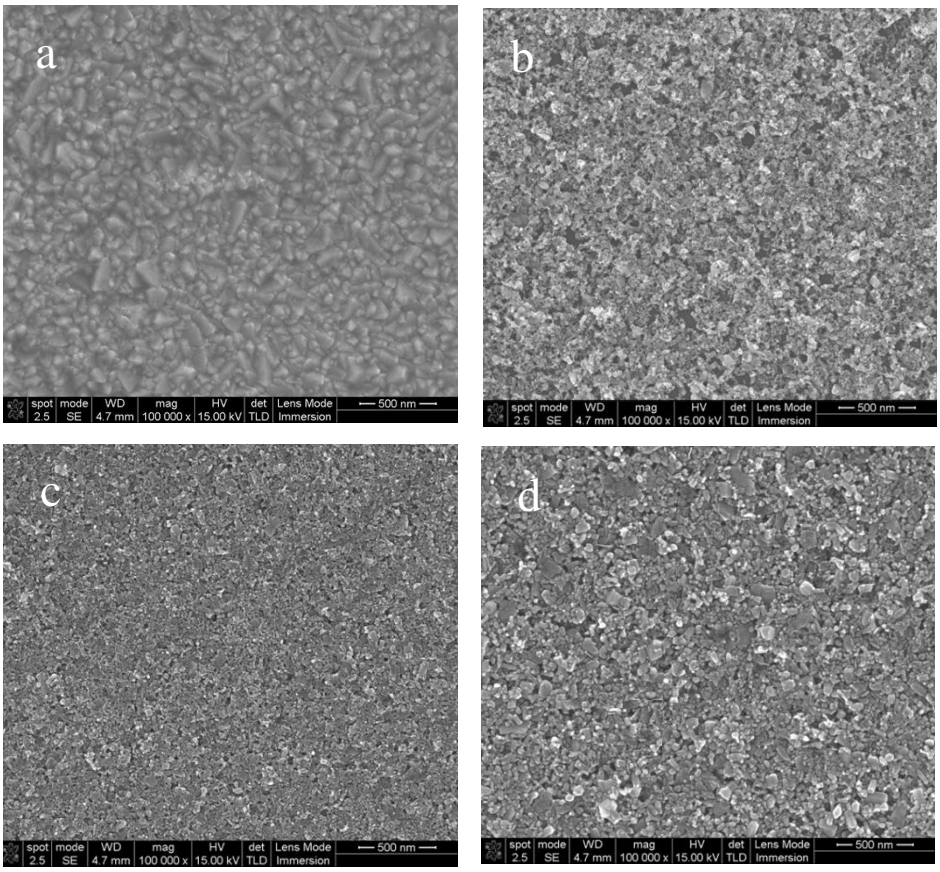

Figure 3.SEM images of AZO films with different Al concentration(a) 0 at.%, (b) 0.3 at.%, (c) 0.7 at.%, and (d)1.2 at.%.

Fig.4 shows the XRD patterns of Al-ZnO thin films annealed to 500 °C. All samples are

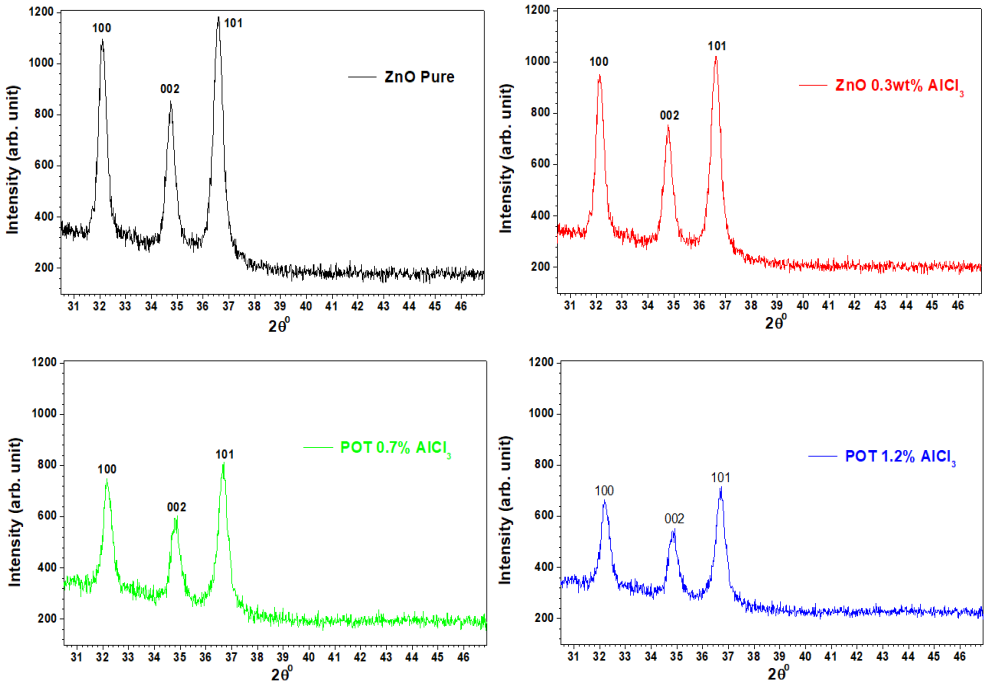

Fig. 4: XRD patterns of AZO films with various Al doping concentrations. All films were annealed to 500 °C in air for 1 h.

polycrystalline and exhibit the hexagonal structure form with preferential (100),(002) and(101) axis orientations with all peaks in the recorded range identified. No other crystalline phase was found within the phase detectability of XRD. As seen in Fig.4, the intensity of the diffraction peaks is decreased, and the FWHM of the peaks is increased with increasing doping concentration, indicating that the film crystallinity is deteriorated. The grain growth of ZnO is promoted by fast diffusion of Zn interstitials at temperatures higher than 350 °C [19]. In the case of trivalent cation doping, the concentration of the zinc interstitials is reduced for charge compensation, resulting in suppressed ZnO grain growth and deteriorated crystallinity [20]. Therefore, the deterioration in crystallinity suggests the incorporation of Al into ZnO. We should notice that this crystallite size as seems much smaller than the grain size as observed in the AFM images. Therefore, although the grain size becomes significantly smaller with increasing Al concentration, the crystallite size only changes slightly. The doping process has more influence on the grain size growth rather on the crystallite size growth. This is probably related with the inhibition of AZO grain growth by the precipitation of $Alcl_3$ on the grain surface [21].

Fig.5 shows the variation of optical transmittance of undoped and Al doped with difference concentrations (0.3, 0.7 and 1.2 at.%) ZnO films on microscope glass substrate. Both undoped and Al doped films exhibit high transparent in the UV-Visible range. The transmittance of Al doped films is in between (82.52-90.97%) in the visible range, which is found to be better than undoped ZnO film. This is may be due to more porous nature of the Al doped film. In the spectra, a sharp absorption transition with absorption edge at around (370nm) nm occurs in the visible region[22].

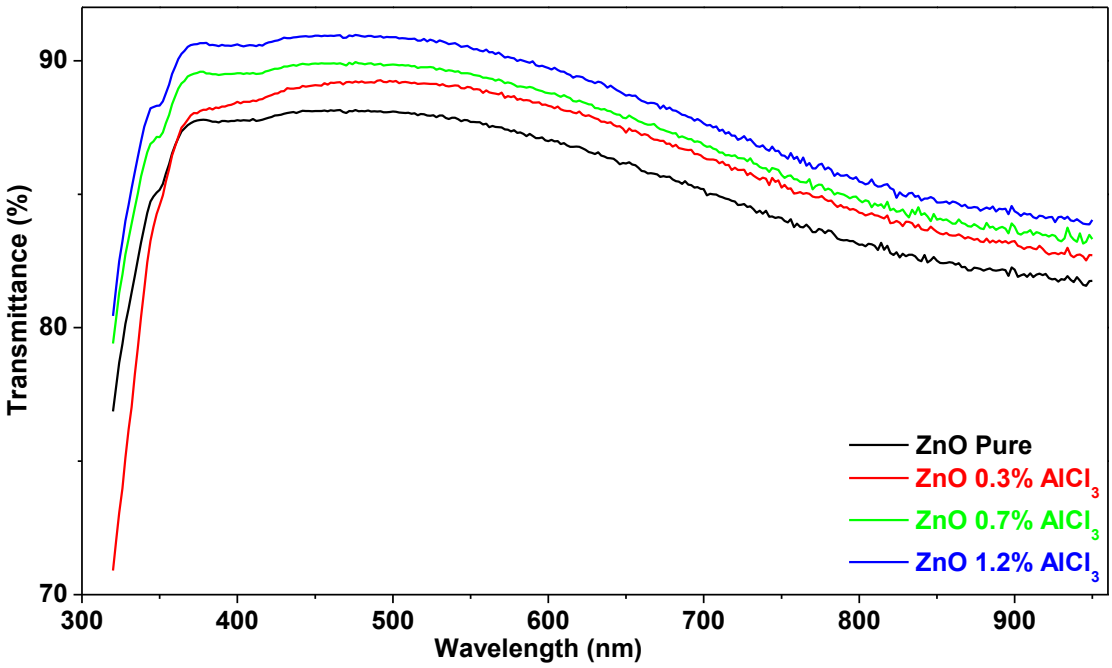

Fig.5: Optical transmittance spectra of AZO films with various Al doping concentrations. All films were

Fig. 6 shows the graph of $(\alpha hv)^2$ vs. photon energy hv for Al-ZO thin films with various Al doping concentrations. The linear dependence of $(\alpha hv)^2$ on hv at higher photon energies indicates that the Al-ZO films are essentially direct-transition-type semiconductors. The straight-line portion of the curve, when extrapolated to zero, gives the optical band gap E_{opt}. From the results of Fig. 6, E_{opt} for the Al-ZO thin films with the Al doping concentration (0, 0.3, 0.7 and 1.2 at. wt%), is (3.34, 3.37, 3.38, 3.41 eV), respectively. This broadening in the band gap is known as the Moss–Burstein shift [23]. According to the Moss–Burstein theory, in heavily doped zinc oxide films, the donor electrons occupy states at the bottom of the conduction band. Since the Pauli principle prevents states from being doubly occupied and optical transitions are vertical, the valence electrons require extra energy to be excited to higher energy states in the conduction band. Therefore, the optical band gap (E_{opt}) of doped zinc oxide is broader than that of undoped zinc oxide films [23,24].

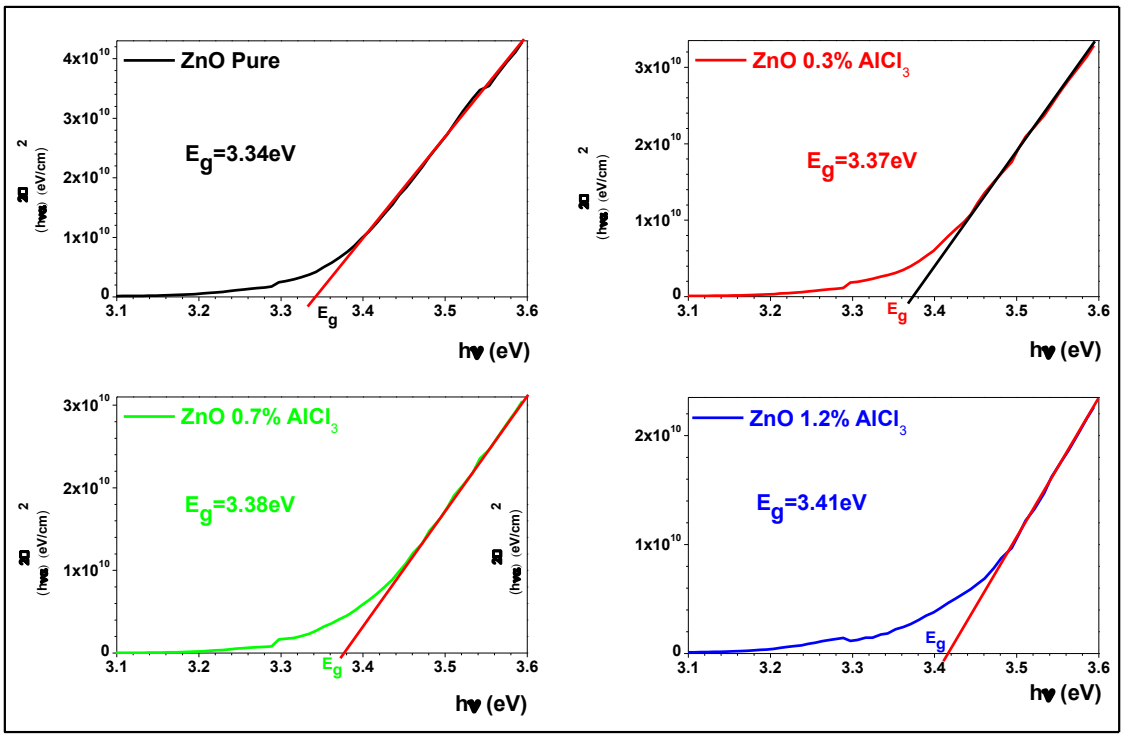

Fig.6. Plots of $(\alpha h\nu)^2$ vs. hυ for AZO films with various Al doping concentrations.

Organic solar cells were then prepared using these Al-ZO layers as its electron transport layer and their characteristics were investigated by J–V. These solar cells were fabricated with ITO/Al-ZO/POT:PC71BM/PEDOT:PSS/Au structure configuration. Fig.7 shows J–V characteristics under light illumination (AM1.5G) measured from these organic solar cells with different doping concentration of Al-ZO layer. All these solar cells produce fairly large short circuit photocurrent density considered for this types of solar cell, namely J_{sc} ~ 3.684–5.139 mA/cm^2. The open circuit voltage (V_{oc}) change remarkably with the variation of Al dopant concentration in Al-ZO layer, where the largest V_{oc} was found is (0.519V) for the solar cell using Al-ZO with 0.7wt %Al dopant concentration. This change in open circuit voltage is suggested to be related to the change of the built-in voltage due to the shifting of AZO Fermi level energy of depending on its Al concentration (0, 0.3, 0.7 and 1.2 at.%). It has been already predicted that up on doping by Al ion the Fermi level energy will be shifted to higher energy to ward into the ZnO conduction band, which is attributed to the Burstein–Moss shift effect [25,26]. As further increase in Al dopant concentration produces larger charge carrier density. It could then be understood that the open circuit voltage becomes larger with increasing Al dopant concentration. The open voltage with Al dopant concentration higher than 1.2 wt%, however, becomes smaller again because of the reduction of charge carrier mobility.

As indicated in Table 1, the FF values, which were a measure of the squareness of J–V curves, nevertheless do not change significantly with Al dopant concentration variation. This may indicates

that the change of J–V characteristics does not originate just from the change of series. However, we may suggest that the variation of J–V characteristics is due to the variation of the ZnO layer junction characteristics, which is also corresponding to the energy level alignment and bending at the junction. The variation of this junction characteristics leads to the efficiency of charge carrier extraction. Fig. 5 shows that the J–V curve of the solar cell with 0.7 wt% Al dopant concentration exhibits the largest area under the J–V curve, indicating the largest charge carrier extraction in comparison to other samples [26-28].

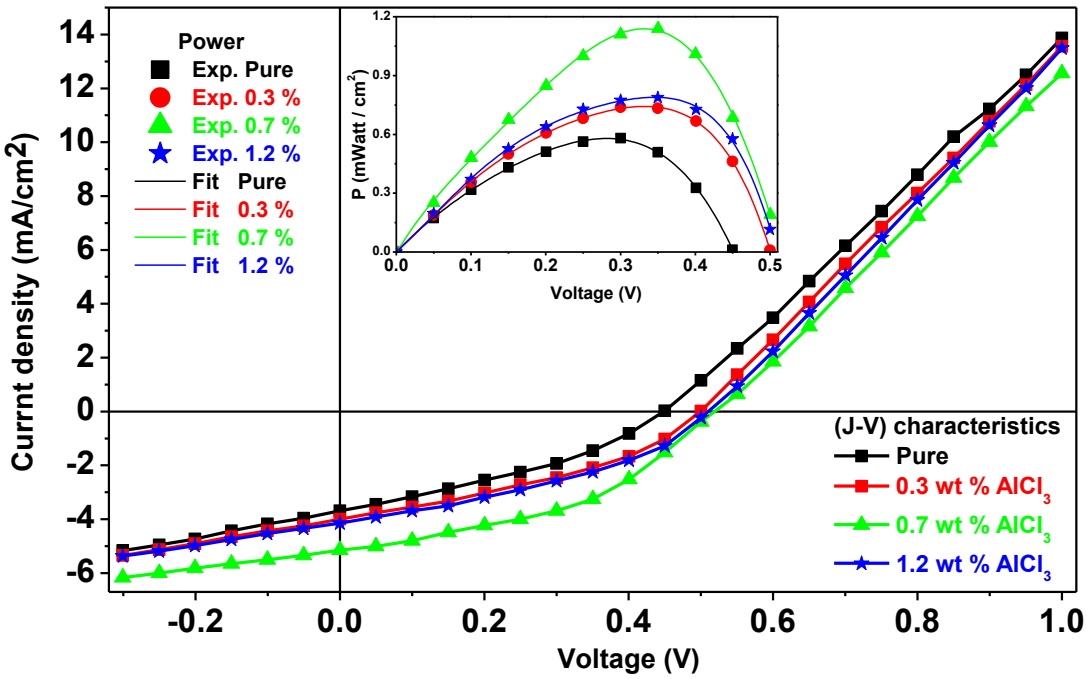

Fig. 7.The J–V characteristics of the fabricated solar cells with undoped ZnO and AZO layers with various dopant concentrations .

Table 1: The solar cell performance parameters determined from the J–V characteristics shown in Fig.7.

Doped wt%	V_{oc} (V)	J_{sc} (mA.cm^{-2})	V_m (V)	J_m (mA.cm^{-2})	*F.F*	η
0.0	0.450	3.684	0.300	1.941	0.352	0.583
0.3	0.500	4.006	0.326	2.273	0.370	0.741
0.7	0.519	5.139	0.336	3.394	0.428	1.140
1.2	0.510	4.139	0.349	2.242	0.371	0.783

4. Conclusions

The fabrications of organic solar cells with inverted structure using POT:$PC_{71}BM$ polymer blend and AZO as their transport layer have been carried out. The AZO layers were prepared by sol–gelroute with various Al concentrations using Isopropyl alcohol as the solvent. From the AFM, SEM, UV-visible and XRD measurements, it was found that the Al concentration has more influence on the grain growth rather than crystallite growth, leading to different surface morphology at different doping concentration. With increasing Al doping concentration, a broadening in the band gap of the AZO films was observed due to the Moss–Burstein shift. A sharp UV peak ascribed to the free exciton emission and defect-related visible luminescence were observed in the AZO films. The J–V characteristics were improved by using AZO layer in comparison to that undoped ZnO layer, where the solar cell with 0.7 wt % Al concentration exhibited the best J–V characteristics among the samples. The open voltage clearly increases with Al concentration in the AZO layer, which can be interpreted as the consequence of Fermi energy shifting in AZO layer to higher energy with increasing Al concentration. These experimental results then indicate that the observed solar cells characteristics are highly correlated with the AZO layer properties, which is influenced by Al dopant concentration.

References

[1] B. Y. Kadem, M. K. Al-hashimi and A, K. Hassan, Materials in Electronics, (2018), 29(9), 7152–7160.
[2] A. Boudrioua, T. Touam, L. Znaidi, D. Vrel, N. Souded, O. Brinza, A. Fischer and S. B. Yahia, Coatings, (2013), 3, 126-139.
[3] J. W. Andreasen, D. M. Tanenbaum, N. Espinosa , M. Jørgensen, F. C. Krebs and H. F. Dam, Materials 2011, 4, 169-182.
[4] S. U. Park and J. H. Koh, Electronic Materials Letters, (2013), 9(4), 493-496.
[5] X. W. Sun, G. Q. Lo, A. K. K. Kyaw, C. Y. Jiang, D. L. Kwong and D. W. Zhao, Applied Physics Letters, (2008), 93, 221107.
[6] D. Manoharan, A. Mahudeswaran, J. Chandrasekaran, P. S. Vijayanand and J. Vivekanandan, Materials Research, (2015), 18(3), 482-488.
[7] C. Drivas, A. Soultati, L. C. Palilis, M. I. Haider, S. Kennou, A. Fakharuddin, E. Polydorou, A. Kaltzoglou, F. Kournoutas, M. Fakis, D. Davazoglou, P. Falaras, P. Argitis, S. Gardelis, A. Kordatos, A. Chroneos, L. S. Mende and M. Vasilopoulou, ACS Appl. Energy Materm (2019), 2(3), 1663-1675.
[8] A. Azarov, L. Liu, Z. Mei, A. Tang, Q. Xue, A. Kuznetsov and X. Du, PHYSICAL REVIEW B (2016), 93, 235305.
[9] P. Samarasekara and U. Wijesinghe, Georgian Electronic Scientific Journals: Physics (2015), 2(14), 41-50.
[10] A. Aprilia, P. Wulandari, V. Suendo, Herman, R. Hidayat, A. Fujii, M. Ozaki, Solar Energy Materials & Solar Cells (2013), 111, 181–188.
[11] O. Edynoor, M.E.A. Manaf , T. Moriga, K. Murai and A.R.M. Warikh, Rev.Adv. Mater. Sci., (2017), 49, 150-15.
[12] V. Musa., B. Teix., E. Fort., R.C.C. Mont., P. Vila., Surf. and Coat. Tech., (2004), 180 –181, 659–662.
[13] Y. Imai, A. Watanabe, Journal of Materials Science: Materials in electronics, (2004), 15, 743–749.
[14] R. Hid., A. Apri., R. Mira., P. Wula., H. H. Wilk., B. Holg., J. Pari., International Symposium on Functional Materials Science, Bali, April 27th– 28th, 2011.
[15] Z.Q. Xu, H. Deng, Y. Li, Q.H. Guo, Y.R. Li, Mate. Rese. Bull, (2006), 41, 354–358.
[16] L., J-Hong; Park, Byu-Ok, Thin Solid Films, (2003), 426, 94-99.
[17] H-ming Zhou, D-qing Yi, Z-ming Yu, L-rong Xiao, J. Li, Thin Solid Films, (2007), 515, 6909–6914.
[18] A. D. Pogr, A. A. Muha, E. T. Kara, N. Y. Jmail, J. Partyka, Prze. Elektrotechniczny, ISSN 0033-2097, R. 89 (2013).
[19] S. Kim, M. S. Kim, G. Nam, and J-Young Leem, Elect. Mate. Lett., (2012), 8, 445-450.
[20] S. Fuji., A. Suzuki, and T. Kimura, Jour. Of Appli. Phys., (2003), 94, 2411.
[21] R. Sidd., R.V. Mang, R. E. Avilab, M. E. Gómezc, D. Mani., M. Lopeza, C. E. Jeyan. and S. Ananthakumar, Jour. of Cera. Proc.Rese., (2012), 13, 801-805.

[22] S. P. Shres, R. Ghim, J. J. Naka, Y-Sung Kim, S. Shres, C-Yun Park, and J-Hyo Boo, Bull. Korean Chem. Soc., (2010), 31, 112.
[23] S-Uk Park and J-HyukKoh, Elec. Mate.Lett, (2013), 9, 493-496.
[24] S. H. Mousavi • T. S. Mu¨ ller • P. W. de Oliveira, Mater Sci: Mater Electron, (2013) 3338–3343.
[25] V. Bhosle, J. T. Prater, F. Yang, D. Burk, S. R. Forrest, and J. Narayan, Jour. of Appl. Phys., (2007), 102, 023501.
[26] J.P. Kar, S. Kim, B. Shin, K.I. Park, K.J. Ahn, W. Lee, J.H. Cho, J.M. Myoung, Solid- State Electronics, (2010), 54, 1447–1450.
[27] E. Barsoukov, J.R. Macdonald, Published by John Wiley & Sons, Inc, Hoboken, New Jersey, ISBN 0-471-64749-7, 2005.
[28] B. Conings, L. Baeten, H. Boyen, D. Spoltore, J. D'Haen, L. Grieten, P. Wagner, M.K.Van bael, J.V. Manca, The Journal of Physical Chemistry C 115 (2011) 16695–16700.